ELSEVIER

Thermochimica Acta 359 (2000) 69–75

thermochimica acta

www.elsevier.com/locate/tca

Thermogravimetric analysis of the ZnO/Zn water splitting cycle

A. Weidenkaff[a,*], A.W. Reller[a], A. Wokaun[b], A. Steinfeld[c]

[a]*Institute of Solid State Chemistry, University of Augsburg, Universitätsstr. 1, D-86159 Augsburg, Germany*
[b]*Department of General Energy Research, Paul Scherrer Institute, CH-5232 Villigen, Switzerland*
[c]*Department of Mechanical and Process Engineering, ETH-Swiss Federal Institute of Technology, CH-8092 Zurich, Switzerland*

Received 14 January 2000; received in revised form 8 March 2000; accepted 31 March 2000

Abstract

The endothermal dissociation of zinc oxide into its elements, followed by the exothermal hydrolysis of zinc, is considered as a two-step water splitting thermochemical cycle using high-temperature solar process heat. Thermogravimetric measurements were conducted on both reaction steps to elucidate the influence of temperature, oxygen partial pressure, inert gas flow rate, and chemical impurities on the reaction kinetics. The dissociation rate increased with the temperature and mass flow rate of an inert gas, and decreased with the oxygen concentration in the inert gas. The hydrolysis reaction proceeded faster for molten zinc and for zinc-containing impurities, but a layer of ZnO prevented reaching completion. The implications on the reactor design are discussed briefly.

Keywords: Solar zinc; Zinc oxide dissociation; Non-stoichiometry; Solar hydrogen; Water splitting

1. Introduction

Hydrogen is an attractive clean fuel when produced from water and the energy required to produce it is obtained from a renewable source, e.g. solar energy. Concentrated solar energy can supply process heat for driving endothermic processes at high temperatures. Water can be split directly using solar process heat via direct thermal dissociation at above 2500 K [1–3]. However, the gaseous products need to be separated at high temperatures for avoiding recombination or otherwise obtaining an explosive mixture. The separation step can be bypassed with the help of thermochemical cycles in which hydrogen and oxygen are generated in different steps. Multi-step thermochemical cycles (more than two) allow the use of more moderate operating peak temperatures also, but their overall energy conversion efficiency is limited by irreversibilities associated with heat transfer and product separation [4].

Two-step thermochemical cycles based on metal oxides offer the potential of achieving high conversion efficiencies while eliminating the need for high-temperature H_2/O_2 separation. Several metal oxide redox systems have been examined and experimentally demonstrated using solar energy [5]. In previous papers [6–8], we reported on a two-step water splitting thermochemical cycle that has the potential of achieving energy conversion efficiencies exceeding 50%. This cycle, shown schematically in Fig. 1, is based on the thermal dissociation of ZnO into its elements according to reaction (1), followed by the exothermic hydrolysis of zinc according

* Corresponding author. Fax: +49-821-598-3002.
E-mail address: anke.weidenkaff@physik.uni-augsburg.de (A. Weidenkaff)

0040-6031/00/$ – see front matter
PII: S0040-6031(00)00508-6

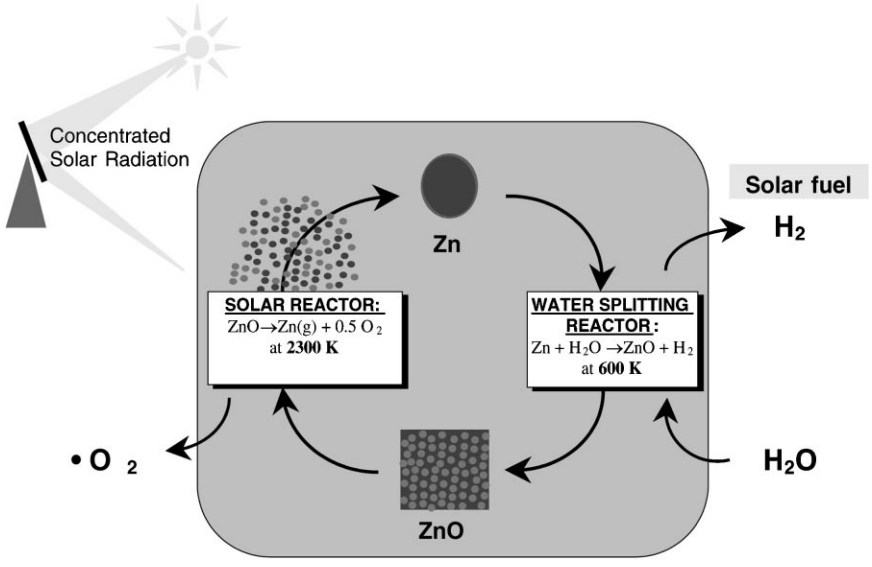

Fig. 1. Schematic representation of a two-step water splitting thermochemical cycle based on the ZnO/Zn redox system. It consists of an endothermic, high-temperature, solar step in which ZnO is reduced to metallic zinc, followed by an exothermic hydrolysis step for the production of solar hydrogen.

to reaction (2):

$$ZnO \rightleftharpoons Zn(g) + 0.5O_2 \quad (1)$$

$$Zn + H_2O \rightleftharpoons ZnO + H_2 \quad (2)$$

Reaction (1) proceeds endothermically ($\Delta H^0 = 478$ kJ/mol) and the temperature for which the equilibrium constant equals 1 is 2350 K [10]. The products, zinc vapour and oxygen, eventually need to be separated to avoid recombination. Thermochromatographic experiments conducted in a temperature-gradient furnace have shown that zinc vapour and oxygen can coexist in a metastable state in the absence of nucleation sites [8]. Reaction (1) has also been demonstrated in solar furnace experiments [3,9,11]. It was observed that the Zn yield is strongly dependent on the dilution ratio of gaseous zinc, defined as the mass flow rate of inert gas divided by the mass flow rate of zinc vapour.

The chemical reaction kinetics of both reaction steps place important initial constraints on the process engineering. In this paper, we investigate the influence of temperature, oxygen partial pressure, inert gas flow rate, particle size, and chemical impurities on ZnO dissociation (reaction (1)), and that of temperature and chemical impurities on zinc hydrolysis (reaction (2)). We further discuss the implications on the reactor design.

2. Experimental

Thermogravimetric measurements were conducted using a Netzsch TASC-419 thermobalance. The experimental setup is depicted schematically in Fig. 2. The furnace consisted of an electrically heated Al_2O_3 tube, 3 cm in diameter, which contained a water-cooled quartz 'cold finger' condenser for trapping Zn vapour. ZnO powder samples (Fluka No. 96479; a mean particle size of 1 μm; a specific surface area, measured by the Brunauer Emmett Teller (BET) method, of 2 m^2/g) were loaded on an alumina flat holder and placed in the thermobalance. Samples were heated at a rate of 50 K/min up to the desired temperature in the range 1273–1823 K, and finally held at isothermal conditions until complete dissociation. Evolved gases were measured on-line by mass spectrometry (MS) and gas chromatography (GC) at the gas outlet of the reactor. The following experimental parameters were varied: N_2 gas flow rate (0–200 ml_n/min[1]), oxygen concentration in N_2 (500 ppm–20%), furnace temperature (1273–1973 K). Zinc yield of the solid products collected on the condenser was deter-

[1] l_n means litres under standard conditions; mass flow rates are calculated at 273 K and 1 bar.

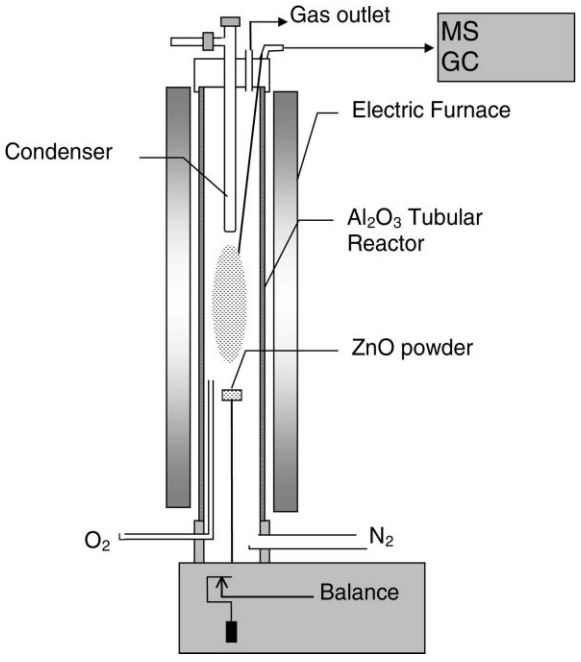

Fig. 2. Thermogravimetric experimental setup for conducting the thermal dissociation of ZnO. ZnO is heated in an alumina crucible. The weight loss is measured on-line. A water-cooled condenser is used for trapping Zn vapour.

mined by X-ray powder diffraction and by measuring the volume of hydrogen evolved when reacted with HCl. It was typically in the range of 40–70 mass% of Zn in ZnO (depending on the oxygen partial pressure in the carrier gas flow). The accuracy of such a technique is ±6% [12].

A similar thermobalance was used for studying the hydrolysis of zinc. Zinc, either commercially purchased or a product from the solar dissociation of ZnO, was placed in an Al_2O_3 crucible, heated to the desired temperature under an N_2 flow, and finally subjected to a 50 ml/min flow of steam-containing N_2 ($p_{H_2O} = 30$, 45 or 50 mbar). The heat absorbed during the melting of zinc (mp 692.7 K) and the heat released due to the exothermic hydrolysis reaction were recorded by differential thermal analysis (DTA). Outlet gases were analysed by a mass spectrometer.

3. Results

3.1. Dissociation of ZnO

Fig. 3 shows the mass loss and furnace temperature as a function of time during the thermal dissociation of ZnO, using a 100 ml/min N_2 flow. The reaction already occurs at 1500 K and reaches reasonable rates at temperatures above about 1700 K. The removal of the gaseous products by the N_2 stream leads to non-equilibrium conditions that favour further dissociation. The temperature dependence of the dissociation rate may be expressed by the Arrhenius law: $k=k_0 \exp(-E_a/RT)$, where k is the rate constant, k_0 the frequency factor (which may also be temperature-dependent, but this effect has been neglected), R the universal gas constant, T the absolute temperature, and where E_a is the apparent activation energy. E_a is determined by fitting the data to the contracting

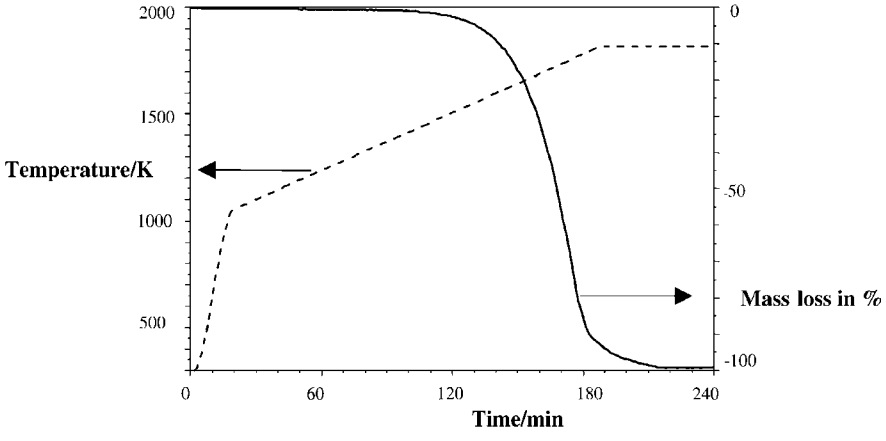

Fig. 3. Mass loss and temperature as a function of time during the thermal dissociation of ZnO.

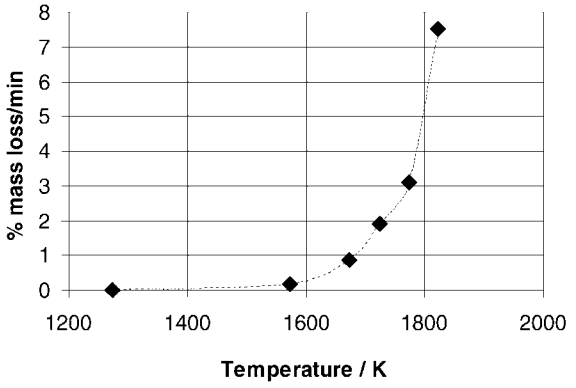

Fig. 4. Variation of the reaction rate with temperature. Samples of ZnO were heated at a rate of 50°/min up to the desired temperature in the range 1273–1823 K, and finally held at isothermal conditions until complete dissociation.

geometry rate law, given by $dx/dt=k(1-x)^n$, where x is the fraction of the solid decomposed at time t obtained from Fig. 3, and n varies between 1/3 and 1, depending on whether the rate-controlling step is a chemical reaction, or gas diffusion, or a combination. The slope of k versus $1/T$ yields an activation energy in the range 312–376 kJ/mol (depending on n), which is consistent with the values reported by [13].

The variation of the dissociation rate with temperature is also shown in Fig. 4. Plotted are the results of TG experiments in which samples were heated to 1273, 1573, 1673, 1723, 1773, and 1823 K, and finally held at isothermal conditions and under a flow of 100 ml_n/min N_2 until complete dissociation.

When ZnO crystals are heated to temperatures above 673 K, oxygen desorbs from the surface, resulting in an increase in excess zinc in the crystal lattice [14]. In experiments conducted in a solar furnace [8], in which samples of ZnO were directly exposed to high-flux solar irradiation, we observed changes in colour, from white to yellow, red, and dark red, due to excess zinc on interstitial sites [15]. Fig. 5 shows a ZnO crystal that has been heated in the solar furnace in air to above 1500 K and that has finally undergone fast cooling. X-ray photoelectron spectroscopy (XPS) analysis revealed excess zinc atoms on the surface of the crystal as a result of oxygen evolution during heating.

Fig. 6 shows the rate of the reaction, expressed in percentage of mass loss per minute at 1723 K, when the N_2 flow rate is 100 ml/min, as a function of the initial mass of ZnO. The reaction rate decreases monotonically as the amount of ZnO increases, probably as a result of the impeded transport of product gases away from the ZnO surface. For the evaluation of specific kinetic data, one has to consider the fact that the absolute values of the reaction rate are strongly dependent on the geometry and morphology of the initial phase.

During the heating of ZnO, the evolution of H_2O and CO_2 was detected at temperatures between 473 and 673 K. ZnO is known to chemisorb H_2O and CO_2 from the atmosphere and form an amorphous surface

Fig. 5. Photo of a red ZnO crystal (3 cm in diameter) with excess zinc in its lattice, obtained by solar heating in air, followed by fast cooling.

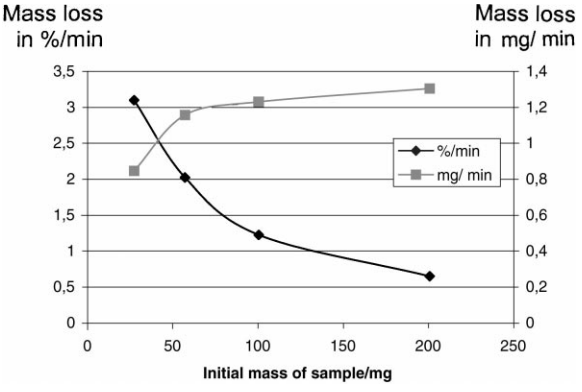

Fig. 6. Influence of the initial geometry (bulk) of the starting material on the reaction rate of ZnO decomposition at 1723 K when the N_2 gas flow rate is 100 ml/min.

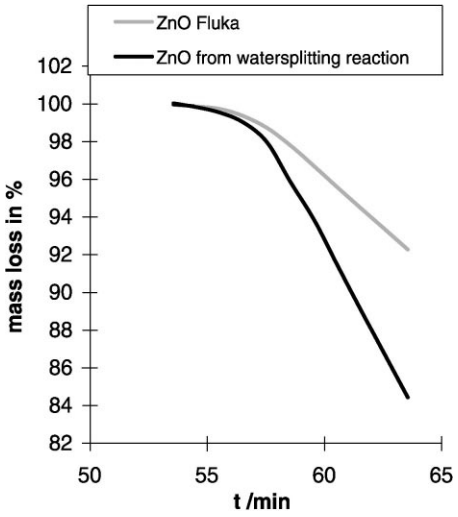

Fig. 7. Comparison of ZnO dissociation for commercial ZnO (Fluka No. 96479) and for ZnO obtained from the hydrolysis of solar zinc (i.e. zinc produced by ZnO dissociation in solar experiments).

product with an approximate composition viz. $Zn_5(OH)_6(CO_3)_2$ [16]. This layer is decomposed during heating under an inert gas flow or vacuum. This partial decomposition leads to a porous structure of the ZnO, with a BET surface area of 6 m^2/g. We also observed that ZnO from different sources had different dissociation rates because the different processes used for ZnO production left various surface impurities; primarily CO_2 and H_2O [17]. Fig. 7 shows the weight loss as a function of time for commercial ZnO (Fluka No. 96479) and for ZnO obtained from the water splitting reaction with solar zinc (i.e. zinc produced by ZnO dissociation in solar experiments). The latter sample dissociates at a faster rate, which may be due to the surface impurities that it contains.

The ZnO dissociation was also effected under various flows of inert gas and various concentrations of oxygen in the inert gas. Fig. 8 shows the dissociation rate at 1723 K as a function of the N_2 mass flow rate. As expected, the reaction proceeded also in a stationary system also, but its rate increases with increasing N_2 gas flow rate as a result of improved transport of gaseous products.

Fig. 9 shows the variation of the reaction rate with O_2 concentration in N_2, at 1773 K. As expected, the reaction rate decreases with increasing oxygen concentration because the presence of oxygen shifts the

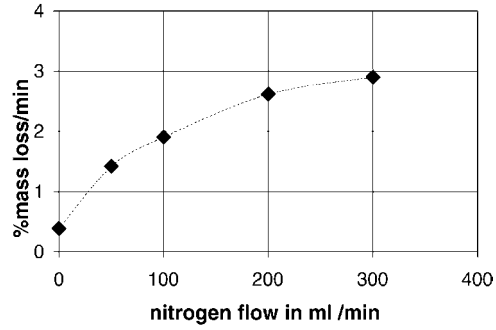

Fig. 8. Variation of the reaction rate with N_2 gas flow rate at 1723 K. Reactor volume is 318 ml.

chemical equilibrium to the left. The reaction proceeds about 10 times faster in inert gas than in air.

In the presence of oxygen, zinc and oxygen recombine to form long whiskers having a dendritic structure on the surface of the ZnO sample, as shown in Fig. 10. Thus, the TG curves obtained are the result of overlapping of the weight loss during ZnO dissociation and the weight gained during the formation of ZnO. It is, however, difficult to discriminate between both reactions because they occur simultaneously.

3.2. Water splitting reaction with Zn

Fig. 11 shows the results of TGA experiments on the reaction of zinc with water vapour. Plotted are the furnace temperature and the weight gain as a function of time for two types of zinc: commercial zinc (Merck No. 108798 with a mean particle size of 10 μm; purity 99%) and solar zinc (a mean particle size of 9 micro-

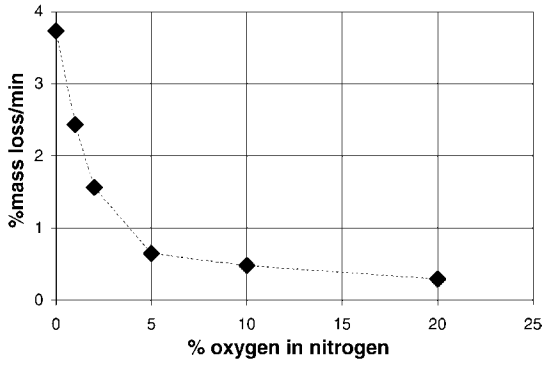

Fig. 9. Variation of the reaction rate with O_2 concentration in N_2 at 1773 K when the gas flow rate is 100 ml_n/min.

Fig. 10. Photo of the ZnO sample after an interrupted dissociation experiment in air.

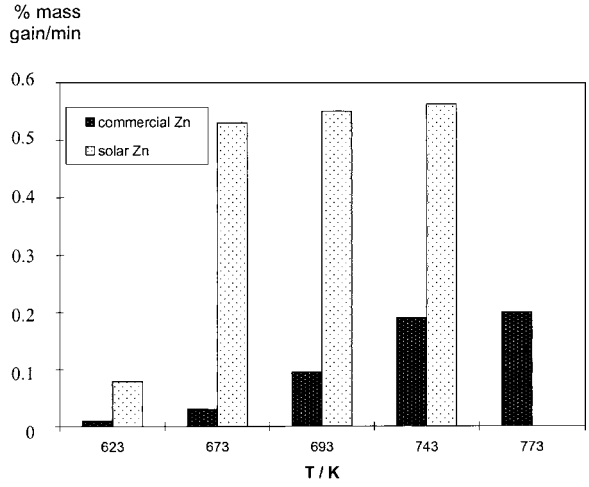

Fig. 12. Water splitting reaction in TGA with 40 mg zinc at 350, 400, 420, 470, and 500°C in a 10.8 mm ∅ vessel, at a nitrogen flow rate of 50 ml/min.

meter; purity 98%) obtained by the dissociation of ZnO in a solar furnace. Fig. 12 shows the reaction rate for various temperatures.

Similar to the oxidation of Zn(l) with O_2 or CO/CO_2 gas mixtures [18], the oxidation of Zn(l) with water depends strongly on the presence of impurities. The reaction rate was found to be only weakly dependent on the water partial pressure, as observed in experiments conducted in the range 30–60 mbar.

Zinc produced in solar experiments contains finely dispersed ZnO impurities [9]; the particle size ranges between 1 and 1.5 μm and its specific surface area is 30 m^2/g. The impurities serve as nucleation sites for further oxidation and function as a 'ZnO matrix' in the reactant. With both samples, the reaction does not achieve completion: the product of experiments with commercial (pure) zinc consisted of black, hard, dense, and sintered material with a zinc content of

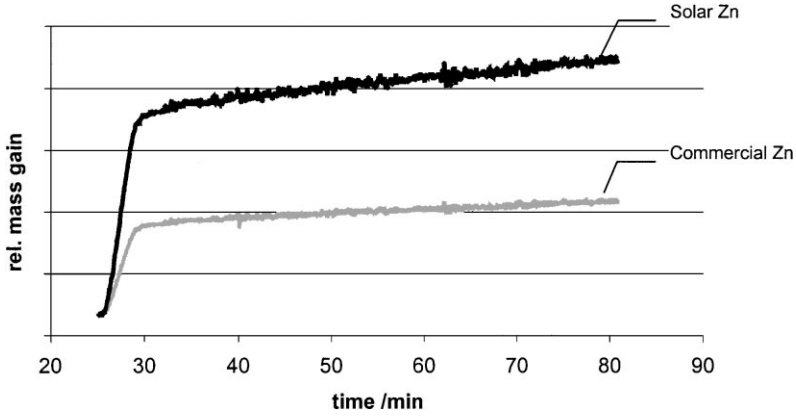

Fig. 11. TGA of the oxidation of zinc with water: comparison of the extent of conversion during the water splitting of commercial and solar zinc.

more than 50%, while the products of experiments with solar zinc consisted of a grey, fine, porous, and voluminous material with a zinc content of less than 10%.

Under the given TG experimental conditions, in which molten zinc in a ceramic crucible is made to react with steam, a ZnO(s) layer is formed and it floats on top of the melt, preventing further reaction. The thickness and density of this layer vary, depending on the impurities and the amount of hydroxyl groups. Complete reaction can be obtained by removing the ZnO layer, by mixing, or by evolving zinc vapour at higher temperatures.

4. Summary and conclusions

We have conducted a set of thermogravimetric experiments to study the effect of various operating conditions on the two reaction steps of a thermochemical water splitting cycle: ZnO dissociation and Zn hydrolysis. As expected, the dissociation rate increased with the temperature and mass flow rate of an inert gas, and decreased with the oxygen concentration in the inert gas. Reaction rates were also faster for samples containing surface impurities. The hydrolysis reaction proceeded faster for molten zinc, but a layer of ZnO prevented reaching completion. Solar zinc containing small amounts of finely dispersed ZnO reacts faster and more completely with water to form hydrogen and ZnO, as compared to commercial zinc samples.

The results of this study place important implications on the reactor and process design. For example, the dissociation reactor will have to be closed to air and operated at temperatures above 1823 K for obtaining an acceptable reaction rate. A flow of inert gas that sweeps the gaseous products will favour dissociation, but it will negatively affect the energy conversion efficiency. Although impurities seem to have a positive effect on both reaction steps, their influence on the cycling capabilities of the process needs to be investigated further. The hydrolysis reactor will have to be operated at above the melting point of zinc and will require good mixing between zinc and water to prevent the formation of a ZnO layer.

Kinetic parameters are interpretable in terms of the experimental conditions chosen. In contrast to the rate constants of reactions in gases or liquids, such parameters include a defined directional component, which has to be in relationship with morphological features [19].

Acknowledgements

This work was enabled through the financial support by the BFE-Swiss Federal Office of Energy.

References

[1] E.A. Fletcher, R.L. Moen, Science 197 (1977) 1050–1056.
[2] A. Kogan, Int. J. Hydrogen Energy 23 (1998) 89–98.
[3] E. Bilgen, M. Ducarroir, M. Foex, F. Sibieude, F. Trombe, Int. J. Hydrogen Energy 2 (1977) 251–257.
[4] C.E. Bamberger, Cryogenics 18 (1978) 170–183.
[5] A. Steinfeld, P. Kuhn, J. Karni, Energy 18 (1993) 239–249.
[6] R. Palumbo, J. Lédé, O. Boutin, E. Ricart, A. Steinfeld, S. Möller, A. Weidenkaff, E.A. Fletcher, J. Bielicki, J. Chem. Eng. Sci. 53 (1998) 2503–2518.
[7] A. Weidenkaff, M. Brack, S. Möller, A. Steinfeld, J. Phys. IV 9 (1999) 313–318.
[8] A. Weidenkaff, F. Sibieude, A. Reller, A. Steinfeld, A. Wokaun, Chem. Mater., in press.
[9] A. Weidenkaff, A. Steinfeld, A. Wokaun, P.O. Auer, B. Eichler, A. Reller, Solar Energy 65 (1999) 59–69.
[10] I. Barin, in: Thermochemical Data of Pure Substances, VCH, Weinheim, 1993.
[11] S. Möller, Diplomarbeit, Paul Scherrer Institut, Villigen, CH, 1997.
[12] P. Widmer, A. Estermann, Semesterarbeit, Paul Scherrer Institut, Villigen, CH, 1997.
[13] W. Hirschwald, F. Stolze, Zeitschr. Phys. Chemie 77 (1972) 21–42.
[14] M.J. Duck, R.L. Nelson, J. Chem. Soc., Faraday Trans. 70 (1974) 436–449.
[15] A.W. Sleight, R. Wang, Mater. Res. Soc. Symp. Proc. 453 (1997) 323–330.
[16] H.R. Oswald, G. Mattmann, F. Schweizer, Helv. Chim. Acta 55 (1972) 1249–1266.
[17] V. Bolis, B. Fubini, A. Reller, J. Chem. Soc., Faraday Trans. 85 (1989) 855–867.
[18] A. Guppy, A.J. Wickens, D.J. Fray, Trans. Inst. Mining Metallurgy 81 (1972) C236–C242.
[19] H.R. Oswald, A. Reller, M. Maciewski, Thermochim. Acta 72 (1984) 139–146.